scientific reports

Check for updates

OPEN

Amyloid fibrils of the myelin basic protein are an integral component of myelin in the vertebrate brain

Evgeniy I. Sysoev[1,2,5], Aleksandr A. Shenfeld[1,4,5], Tatyana A. Belashova[1,3], Anna A. Valina[1,2], Sergey P. Zadorsky[1,2] & Alexey P. Galkin[1,2]✉

The myelin basic protein (MBP) is the most abundant intracellular protein of the myelin, which forms the electrically insulating sheath of axons of many actively functioning neurons. This protein binds the opposite membranes of the flattened processes of oligodendrocytes and plays a crucial role in myelin compaction. Here we show that MBP is present in amyloid form in the oligodendrocytes in the brain of vertebrates. It forms SDS-resistant insoluble aggregates and clearly colocalizes with Congo Red and Thioflavin S in vivo, ex vivo, and in vitro. The fibrils of MBP extracted from the brain are detected by electron microscopy and exhibit apple-green birefringence after Congo Red staining. We showed that the central region of MBP, spanning amino acid residues 60–119, is responsible for the formation of amyloid fibrils. Based on these data, we present a model in which MBP not only connects the opposite membranes of oligodendrocyte processes but also provides longitudinal amyloid stitching of myelin sheaths. Amyloid fibrils appear to be an ideal natural material for myelin compaction and axon insulation.

Keywords Brain, Myelin, Myelin basic protein (MBP), Functional amyloid, Fibrils, Oligodendrocytes, Axonal insulation

Myelin is an electrically insulating sheath around axons of many neurons, ensuring the rapid and efficient conduction of nerve impulses. These sheaths are formed by Schwann cells in the peripheral nervous system and by the flattened processes of oligodendrocytes in the brain[1,2]. Central nervous system (CNS) myelination is typically divided into an intrinsic and adaptive phases[3]. The intrinsic phase of myelination, which is genetically determined and affects strictly defined groups of axons, occurs in the early stages of development[4]. Recent studies have shown that adaptive myelination depends on experience and external influences in the course of individual development[5]. Since myelination determines conduction velocity, disturbances in this process affect memory, learning, and reaction rate. Inflammatory demyelinating diseases cause neurodegenerative lesions of the CNS[6].

Each oligodendrocyte generates several processes that can bind axons of different neurons. These processes recognize the axons of actively functioning neurons and wrap around them. Multiple long myelinated sections are separated from each other by short gaps called nodes of Ranvier. The alternation of compact myelin sheaths with Ranvier intercepts containing sodium/potassium ion channels in discrete locations provides faster action potential propagation by saltatory conduction[7,8]. The formation of the myelin sheath around the axon is accompanied by the flattening of the oligodendrocyte processes and the formation of an intracellular "major dense line" and the "intraperiod line". The major dense line is formed throughout the entire sheath, excluding the inner layer that contacts the axon and the outer layer.

The mechanism of myelin compaction remains a mystery. The myelin basic protein (MBP) plays a key role in myelin compaction and displaces other proteins out of the flattened processes[9]. It is the most abundant intracellular protein in oligodendrocyte processes existing in several isoforms[10]. Deletion of a large fragment of MBP in mice leads to significant demyelination and prevents compact myelin formation. Mice carrying this deletion exhibit axonal conduction deficits, progressive tremor and ataxia, seizures, and shortened lifespan[11,12]. The mRNA of MBP is transported along microtubules to the cell periphery, where it is translated[13]. MBP binds lipid membranes through electrostatic interactions between its basic residues and the negatively charged

[1]St. Petersburg Branch, Vavilov Institute of General Genetics, Russian Academy of Sciences, Universitetskaya Emb. 7/9, 199034 St. Petersburg, Russia. [2]Department of Genetics and Biotechnology, Faculty of Biology, St. Petersburg State University, Universitetskaya Emb. 7/9, 199034 St. Petersburg, Russia. [3]Laboratory of Amyloid Biology, St. Petersburg State University, Universitetskaya Emb. 7/9, 199034 St. Petersburg, Russia. [4]Present address: Skolkovo Institute of Science and Technology, Bolshoy Boulevard, 30, Bld.1, 121205 Moscow, Russia. [5]Evgeniy I. Sysoev and Aleksandr A. Shenfeld have contributed equally to this work. ✉email: a.galkin@spbu.ru

head groups of the inner leaflet of membrane lipids[13,14]. The N- and C-termini of MBP independently interact with opposite membranes[14,15]. The binding of intrinsically unstructured MBP to membranes results in major conformational changes and self-assembly[15]. These events lead to the formation of a 3 nm wide major dense line between two lipid bilayers. The mechanism of conformational transitions and aggregation of MBP remains unknown. Mikael Simons and colleagues suggested that myelin compaction is accompanied by the formation of MBP amyloid-like fibrils. They demonstrated that the corpus callosum in wild-type mice was stained with the amyloid-specific dye Thioflavin S (ThS), whereas the corresponding brain area in mice with MBP deletion was not. The authors also showed that MBP and its fragments can form fibrillar structures[16]. However, the authors did not study the amyloid properties of these fibrils. In another study, MBP isolated from the rat brain was found in the fraction of detergent-resistant amyloid-like aggregates[17]. Given the fact that myelin insulates axons, the hypothesis that MBP forms a network of compact amyloid fibrils is highly appealing.

Here we perform a detailed analysis of the amyloid properties of MBP in the brain and in vitro. Based on the obtained data, we present a model in which amyloid fibrils are an integral component of myelin sheaths.

Results

MBP is present in the brain in the form of SDS-resistant oligomers and aggregates

Previously, using proteomic screening, we identified the MBP protein in the fraction of detergent-resistant aggregates in the rat brain, suggesting that this protein may form amyloid-like aggregates[17]. To test whether MBP actually forms detergent-resistant amyloid-like aggregates in vivo, we used the semi-denaturing agarose gel electrophoresis (SDD-AGE) method[18]. The data presented in Fig. 1a demonstrate that MBP predominantly remains in the form of aggregates after treatment of rat brain lysate with 1% sodium dodecyl sulfate (SDS) at room temperature (Fig. 1a and Supplementary Fig. S1). The fractionation method was then used to analyze the comparative ratio of monomers, oligomers, and insoluble aggregates of MBP in rat brain. For this experiment, brain lysate was separated into three fractions after incubation in 1% SDS: 1—proteins present in the fraction with a molecular weight of less than 30 kDa; 2—soluble proteins with a molecular weight of more than 30 kDa; and 3—high molecular weight protein aggregates detected in the insoluble sediment fraction (Fig. 1b and Supplementary Fig. S2). Using MBP-specific antibodies, we demonstrated that the major isoforms of this protein are detected in oligomeric and aggregated fractions, whereas MBP in monomeric form was undetectable. The presented results indicate that all MBP isoforms, as well as known amyloids, form detergent-resistant aggregates.

In the brain, MBP colocalizes with amyloid-specific dyes

According to earlier studies, bundles of myelinated axons in the brains of healthy mice are stained with amyloid-specific dye ThS[16]. Moreover, no dye binding was observed in the brains of *shiverer* mice with deletion of a significant part of the *MBP* gene. To assess whether MBP exists in the rat brain in amyloid form, we evaluated the colocalization of MBP with the amyloid-specific dyes in adult rat brain cryosections (Fig. 1c,d). Our data show that MBP colocalizes in the myelin sheaths of the rat striatum with ThS (Fig. 1c). We also detected colocalization of MBP with ThS in the brains of representatives of different classes of jawed vertebrates, such as the common frog *Rana temporaria*, the red-eared slider *Trachemys scripta elegans*, and the chicken *Gallus gallus domesticus* (Supplementary Fig. S3). It should be noted that ThS can stain not only amyloids, but also, in some cases, structures of non-amyloid nature[19]. In this context, we also assessed the colocalization of MBP with the amyloid-specific dye Congo Red (CR). The location of MBP in the rat brain matched exactly the CR signal (Fig. 1d). Moreover, we observed apple-green birefringence under crossed polarized light (Fig. 1e) after such staining, which is a characteristic feature of amyloids[20]. These data indicate the presence of amyloid fibrils in the myelin sheaths of a healthy adult rat. Taken together, the data on colocalization of MBP with amyloid-specific dyes in the brain suggest that this protein can function in the brain in amyloid form.

MBP isolated from rat brain has amyloid structure

The data on the colocalization of MBP with amyloid-specific dyes and its ability to form SDS-resistant aggregates are insufficient to confidently speak about the amyloid properties of this protein. In addition to MBP, other proteins are present in myelin sheaths[21]. Moreover, some proteins form detergent resistant non-amyloid aggregates[22].

To obtain conclusive evidence for the amyloid nature of MBP, we focused on evaluating the amyloid properties of this protein isolated from the brain by immunoprecipitation using commercially available anti-MBP antibodies. To isolate of pure MBP fibrils with minimal contamination we used the method described previously[23] with modifications (see "Materials and methods"). An aliquot of the eluate was boiled and analyzed by Coomassie gel staining and immunoblotting. Two major bands, corresponding in size to the 14 and 18.5 kDa MBP isoforms, were detected on the Coomassie-stained gel (Fig. 2a and Supplementary Fig. S4). Immunoblotting confirmed that these protein bands represent MBP isoforms (Fig. 2b and Supplementary Fig. S5). Thus, using immunoprecipitation, we obtained purified preparations of the MBP protein from the brain. As shown in Fig. 2c, MBP immunoprecipitated from the brain binds CR and exhibits apple-green birefringence under crossed polarized light. Furthermore, transmission electron microscopy (TEM) imaging combined with immunogold labeling (see "Materials and methods") verified that the isolated fibrils contain MBP (Fig. 2d). These data provide definitive evidence of the amyloid nature of the MBP protein.

The central region of the MBP protein is responsible for its aggregation

Using the bioinformatic approach AmylPred2[24], which combines the prediction results of several independent programs, the amyloidogenic motif PVVHFFKNI was found to be present in all isoforms of rat MBP. Moreover, a comparative analysis of the amyloidogenic region predictions in all MBP isoforms from different representatives of jawed vertebrates, ranging from cartilaginous fishes to humans, revealed a consensus VVHFF sequence

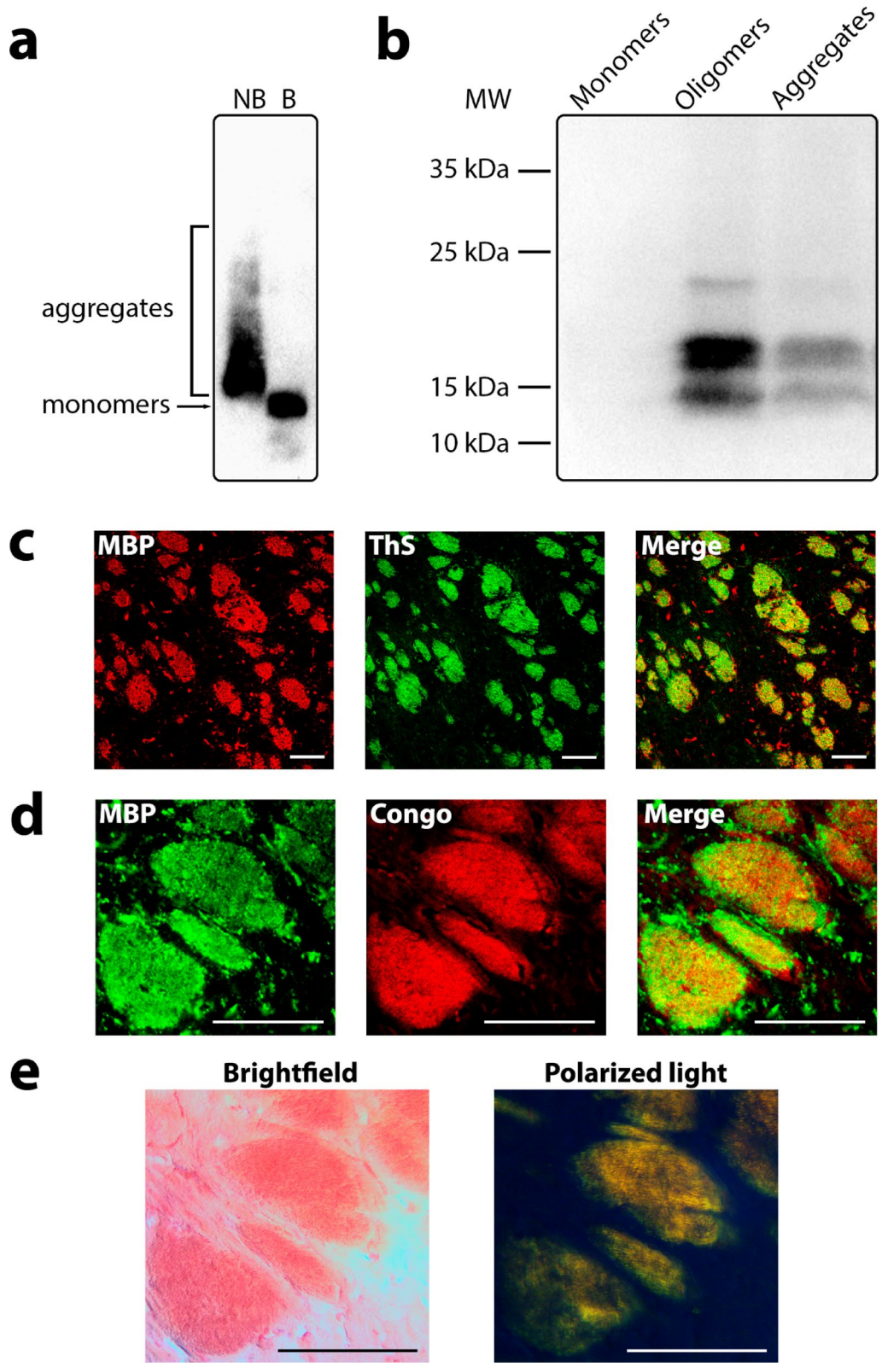

Fig. 1. Biochemical and immunohistochemical analysis of the amyloid properties of the MBP protein in the rat brain. (**a**) Detection of SDS-resistant MBP aggregates isolated from the brain using the SDD-AGE method. NB–nonboiled sample, B–boiled sample. (**b**) Analysis of the SDS-resistance of the rat brain MBP by the fractionation method. Protein lysates were separated into an insoluble sediment fraction and fractions containing MBP monomers and oligomers. (**c**), (**d**) Colocalization analysis of MBP with amyloid-specific dyes ThS (**c**) and CR (**d**) in the striatum of rat brain using confocal microscopy. Scale bar, 50 µm. (**e**) CR staining of myelinated fiber bundles under transmitted (brightfield) and crossed polarized light. Scale bar, 50 µm.

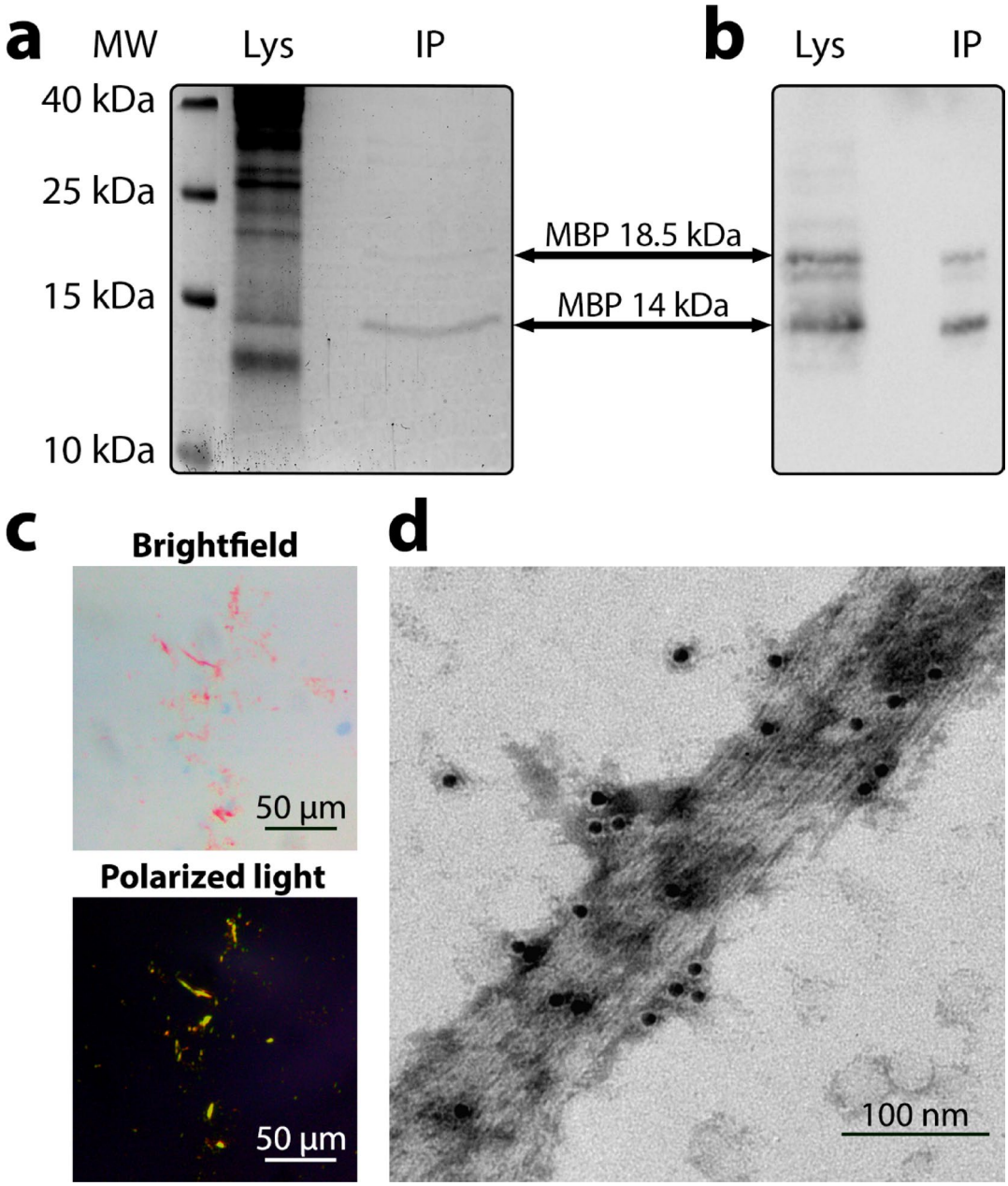

Fig. 2. Immunoprecipitation of MBP fibrils from rat brain. (**a**) Coomassie-gel staining and (**b**) immunoblotting of MBP after immunoprecipitation. Lys–clarified brain lysate; IP–immunoprecipitate. (**c**) Staining of isolated MBP with CR. (**d**) Negative-stain electron microscopy images of the purified immunogold labeled MBP fibrils isolated from a rat brain. PAA539Mi01 was used as a primary rabbit anti-MBP antibody. A goat anti-rabbit gold-conjugated antibody with a gold particle (10 nm) was used as a secondary antibody.

(Fig. 3). However, it should be noted that the data obtained from bioinformatic algorithms are only predictive and require experimental validation. Moreover, there are serious reasons to believe that a short sequence consisting of only five or nine amino acid residues cannot ensure amyloid aggregation of a full-length protein[25].

To identify the amyloidogenic region, we used a yeast model system. We obtained a set of plasmids for expression of different fragments of MBP fused to yellow fluorescent protein (YFP). It should be noted that the following amino acid numbering in the MBP protein corresponds to that of the 17.22 kDa MBP isoform. First, we evaluated the aggregation of the N-terminal fragment of MBP (1–59 amino acid residues), corresponding to the mutant *shiverer* protein form, which is characterized by the deletion of part of the exon II and the sequence spanning exons III to VII of the *MBP* gene[26]. This fragment fused to YFP does not form visible aggregates in yeast cells (Fig. 4a). The chimeric protein containing MBP sequence from 60 to 154 amino acid residues forms multiple bright fluorescent foci (Fig. 4a). A similar aggregation pattern is observed with the chimeric MBP(60-119)-YFP protein, which contains a shorter MBP fragment (Fig. 4a). These data are consistent with the prediction results of the AmylPred2 algorithm, as the potentially amyloidogenic PVVHFFKNI fragment is located in the

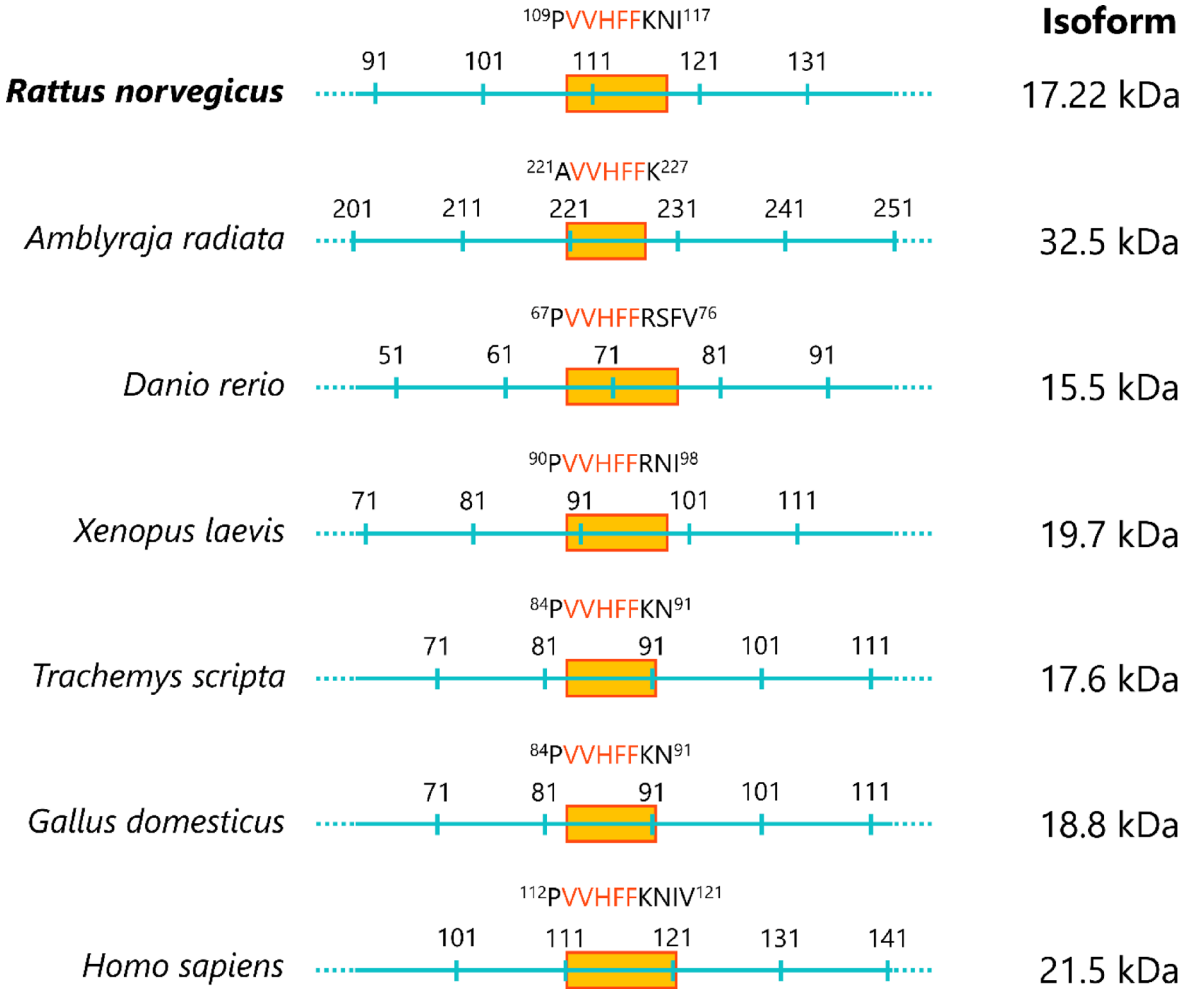

Fig. 3. Bioinformatic search for the amyloidogenic regions in MBP across representatives of evolutionarily distant groups of jawed vertebrates using the AmylPred2 approach. The figure illustrates the location (a yellow rectangle) of the potentially amyloidogenic sequence. The consensus sequence is indicated in red. Corresponding protein sequences were obtained from the NCBI data repository (https://www.ncbi.nlm.nih.gov/search/).

109 to 117 amino acid residues region of the 17.22 kDa isoform. However, our data show that MBP(86–119) fragment, which also contains this sequence, does not form visible aggregates and is uniformly distributed in the yeast cytoplasm (Fig. 4a). The MBP protein with a deletion of the central fragment (amino acid residues from 60 to 105) shows uniform fluorescence, further supporting the importance of the central region of the protein in aggregation (Fig. 4a). Moreover, the 17.22 kDa isoform of MBP forms aggregates in yeast cells, whereas the 14 kDa isoform lacking amino acid residues 60 to 85 encoded by exon II shows uniform fluorescence. These data show that the presence of the MBP(86–119) fragment including potentially amyloidogenic PVVHFFKNI peptide is essential but insufficient for aggregation of the protein in vivo. The fragment comprising amino acid residues 60-119 is also required for MBP aggregation. The aggregation frequencies of all proteins containing the MBP(60-119) fragment exceed 90%. Chimeric proteins that do not contain the MBP(60-119) sequence did not form aggregates in the analyzed cells. (Supplementary Fig. S6, Supplementary Table S2).

We then assessed the amyloid properties of chimeric proteins containing the MBP fragments from 60 to 119 amino acid residues. The yeast cell wall contains some amyloid proteins that are stained with amyloid-specific dyes[27–29]. This prevents the detection of intracellular amyloids in yeast cells. We mechanically disrupted the cells and removed most of the cell wall using low-speed centrifugation (see "Materials and methods"). Cell lysates containing the chimeric proteins MBP(17.22 kDa)-YFP and MBP(60-119)-YFP were stained with ThS dye. ThS and YFP have partial overlapping emission spectra. Therefore, we selected detection wavelengths under which only ThS or YFP is detected (see "Materials and methods"). All detected MBP-YFP and MBP(60-119)-YFP aggregates colocalize with ThS (Fig. 4b). Thus, chimeric proteins containing MBP fragments from 60 to 119 amino acid residues exhibit amyloid properties in yeast cells.

To further confirm our results, we analyzed the amyloid properties of MBP fragment comprising amino acids 60 to 119 in a cell-free in vitro system. We have analyzed the aggregation kinetics of MBP(60-119) using the amyloid-specific dye Thioflavin T (ThT) (Fig. 5a, Supplementary Table S1). The maximum ThT fluorescence

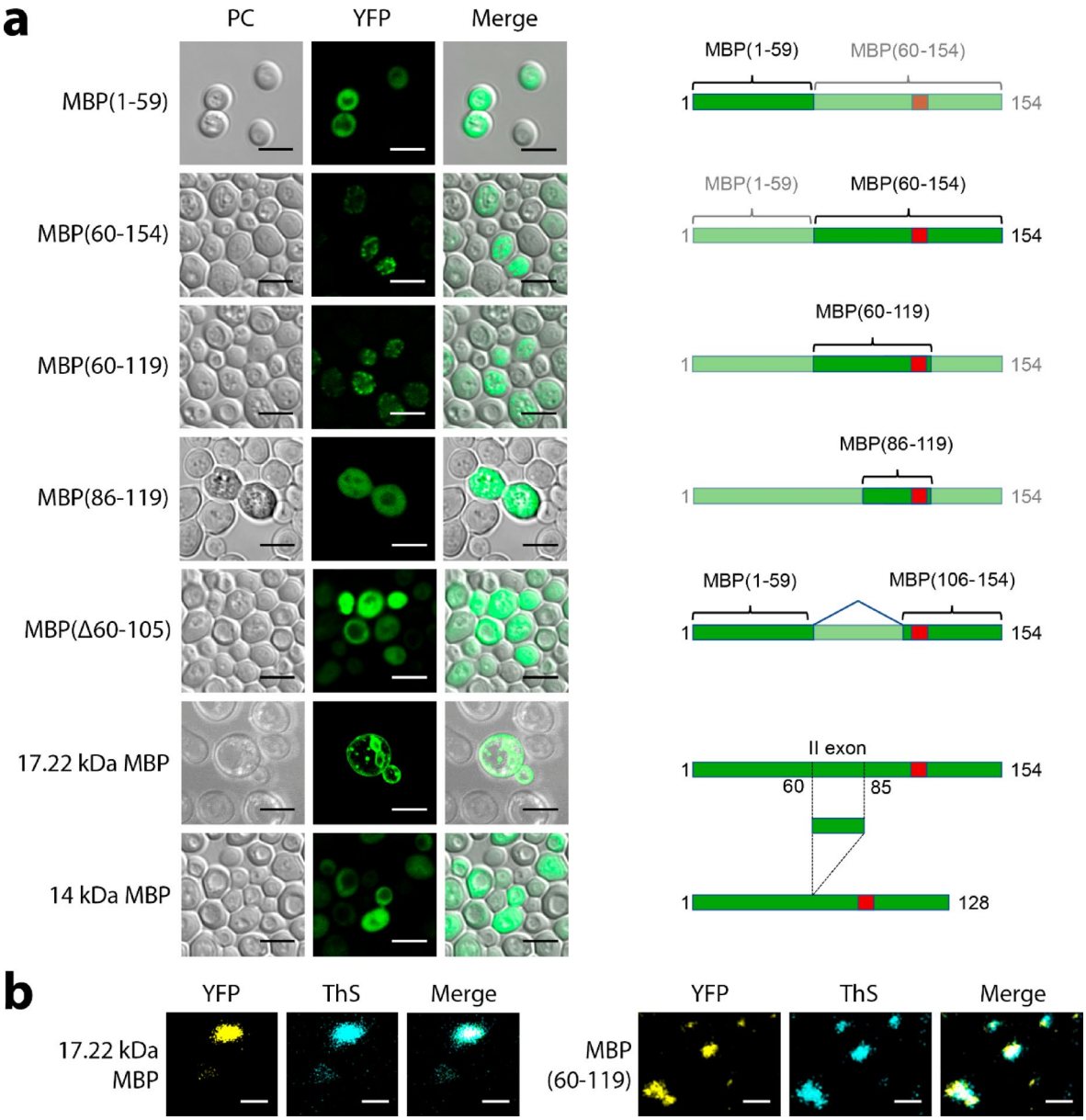

Fig. 4. Analysis of aggregation of MBP fragments and its full-length isoforms fused to YFP in yeast model system. (**a**) Aggregation of full-length isoforms of MBP and its fragments in yeast cells. On the right is a schematic representation of MBP sequences (indicated in green) in each chimeric protein included in the analysis. Pale green indicates regions of the MBP sequence that are not included in the respective fragment. The red square indicates a potentially amyloidogenic region. Scale bar, 5 µm. (**b**) Colocalization analysis of yeast-derived MBP(17.22 kDa)-YFP and MBP(60-119)-YFP with the amyloid-specific dye ThT. Scale bar, 2 µm.

at the aggregation plateau was observed after approximately 30 h of incubation under physiological conditions. Addition of 5% pre-existing aggregates to the MBP(60-119) peptide accelerates fibril formation. The statistical significance of this difference was confirmed based on the results of five experimental replicates (Fig. 5b). To analyze the capacity of MBP(60-119) to form the fibrillar structure, this peptide was incubated in PBS for five days as described in the "Materials and methods" section. After incubation, TEM revealed well-defined 12 nm filaments twisted into fibrils and forming layers (Fig. 5c–e). MBP fibrils are stained with Congo Red and exhibit birefringence (Fig. 5f). Our results are in good agreement with studies of the aggregation of known amyloids, such as Aβ[30] and α-synuclein[31], in vitro.

Taken together, our data show that the MBP protein forms amyloid fibrils in myelin sheaths, and that MBP(60-119) fragment is essential for its aggregation.

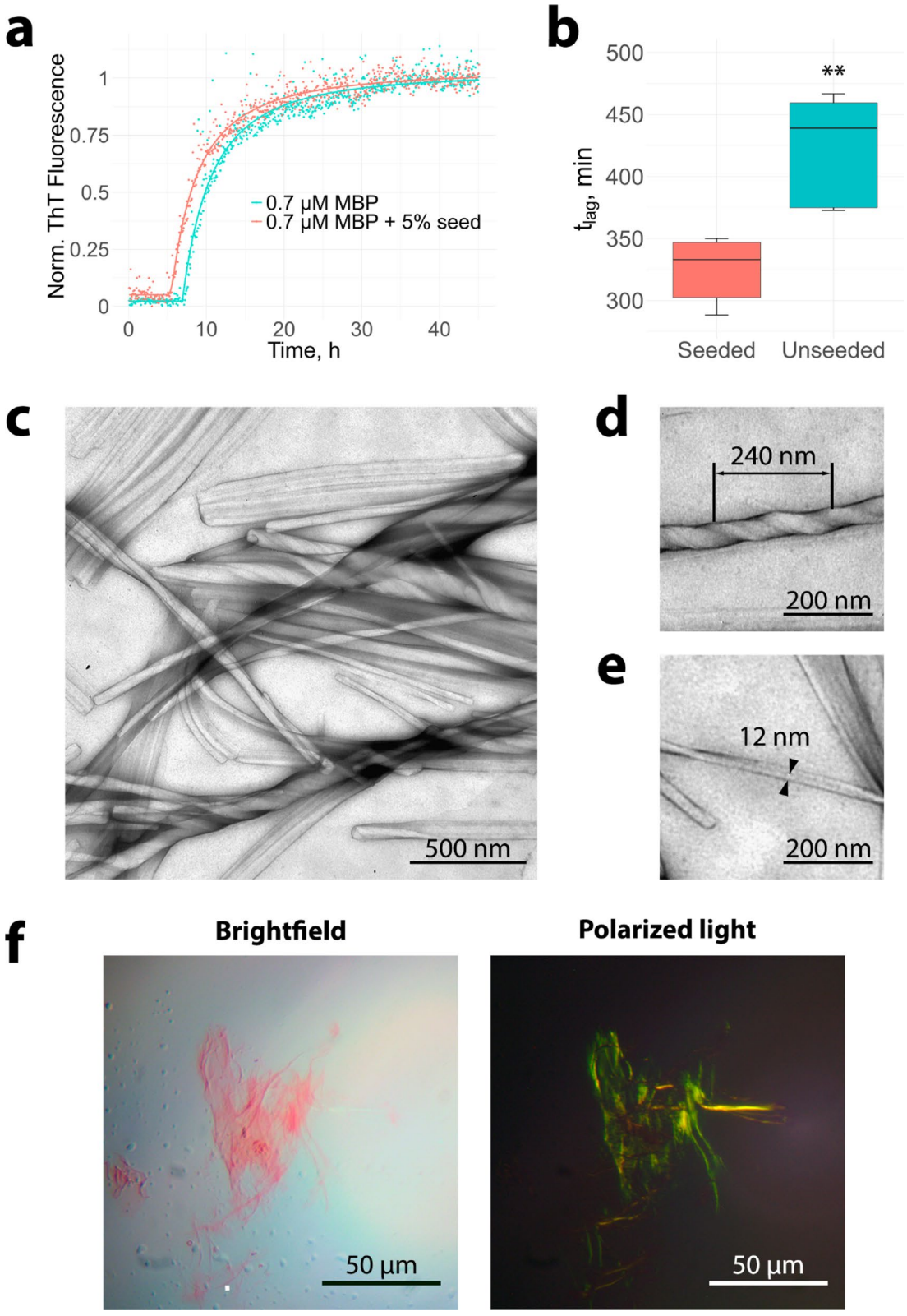

Fig. 5. Analysis of amyloid properties of MBP(60-119) fragment in vitro. (**a**) Kinetic curve of amyloid aggregation of MBP(60-119) in the presence (red curve) and absence (blue curve) of 5% seed. (**b**) Statistical difference between the lag phase time of seeded and unseeded experiments. (**c**)–(**e**) TEM analysis of the MBP(60-119) peptide: (**c**) the filaments of MBP form sheets or bundles; (**d**) the fibrils have twist pattern; (**e**) the individual filaments are approximately 12 nm thick. (**f**) CR staining of MBP(60-119) fibrils and birefringence under crossed polarized light.

Discussion

We have shown that the MBP protein, which plays a key role in myelin compaction, forms amyloid fibrils in vivo and ex vivo. In brain sections, MBP colocalizes with the amyloid-specific dyes ThS and CR. Areas stained with CR exhibit apple-green birefringence, a characteristic feature of all classical amyloids. MBP isolated from rat brain by immunoprecipitation is presented in the form of amyloid fibrils. Amyloid fibrils of MBP appear to be an ideal natural material for myelin compaction and axon insulation, facilitating the effective conduction of nerve impulses.

Our data from the yeast model system indicate that a fairly extended central region containing amino acid residues from 60 to 119 is responsible for MBP aggregation. The data from a heterologous system should be treated with caution, but this fragment has also been shown to form amyloid fibrils in vitro. Using electron microscopy, we observed individual filaments with a diameter of approximately 12 nm, which were assembled into sheets or bundles with a characteristic twist pattern. These properties were found in all previously described fibrils with a cross-β structure.

These results are in good agreement with the literature data, according to which the N- and C-terminal sequences of MBP bind to lipids in the membranes of flattened processes of oligodendrocytes located opposite each other[14]. Interestingly, the 17.22 and 21.5 kDa isoforms contain the amyloidogenic fragment MBP(60-119), whereas the 14, 17.24, and 18.5 kDa isoforms lack the part of this sequence (amino acid residues 60 to 85) corresponding to exon II[10]. At the same time, our data show that all MBP isoforms form SDS-resistant oligomers and high-molecular aggregates in the rat brain (Fig. 1). As noted above, all MBP isoforms contain the short, potentially amyloidogenic, sequence PVVHFFKNI. Probably, the 17.22 and 21.5 kDa isoforms act as seeds for the aggregation of other MBP isoforms.

Opposite membranes of oligodendrocyte processes do not differ from each other, and it could be assumed that the protein monomers attach to the membrane in a random orientation. However, we showed that MBP forms amyloid fibrils, which completely excludes the possibility of random orientation of the protein monomers. Amyloid fibrils have either a "parallel in-register" or "antiparallel" structure[32]. In the first case, all monomers within a fibril are oriented parallel to each other, while the antiparallel structure of the fibrils implies a strict alternation of monomers in direct and opposite orientations. Random orientation of monomers within a single fibril is impossible. Determining monomers orientation through structural analysis of MBP fibrils presents a challenge for future research. However, based on the analysis of MBP(60-119) sequence, we can reasonably assume that the molecules of this protein are likely to form fibrils with an antiparallel structure. This sequence is enriched in charged amino acid residues (14 positively and three negatively charged amino acid residues). Known sequences that form parallel in-register amyloid tracts usually consist of uncharged amino acid residues, as repulsion of equally charged groups prevents the formation of a cross-β structure. However, in the case of antiparallel orientation, fairly long tracts can form where similarly charged amino acid residues are not located opposite each other. Possible variants of such MBP tracts are presented in the Supplementary Materials (Supplementary Fig. S7). Based on our data, we present a model reflecting the role of MBP in the formation of myelin sheaths. According to our model, MBP not only links the opposite membranes of oligodendrocyte processes, but also provides longitudinal amyloid stitching of myelin sheaths (Fig. 6).

Overall, we obtained clear evidence that MBP exists in amyloid form in the brain. Amyloid fibrils may contribute to the compaction of myelin and the insulation of axons. Taking into consideration the unique properties of amyloid fibrils, it is not surprising that, during evolution, vertebrates began to use these structures to form insulating myelin sheaths. Our data show that amyloid may play an important role in the structural organization of the brain's white matter.

Materials and methods

Animals, brain slice preparation, and brain homogenization

Four-month-old male Wistar rats were purchased in Rappolovo laboratory animal nursery (Saint-Petersburg, Russia). Domestic chickens (*Gallus gallus domesticus*) of the Russian White breed, aged 6–12 months, were purchased from the All-Russian Research Institute of Genetics and Farm Animal Breeding "Genofond" (Pushkin, Leningrad Region, Russia). Mature adults of common frog *Rana temporaria* and red-eared slider *Trachemys scripta* were purchased from breeders. All animal experiments were conducted in accordance with relevant guidelines and regulations and ARRIVE guidelines. Experiments were approved by the Ethical Committee for Animal Research of St. Petersburg State University (Statement #131–03-6 issued 01.06.2017). Euthanasia of animals was performed by injection of zoletil followed by decapitation. Euthanasia of animals was carried out immediately after delivery to Saint Petersburg State University.

For immunohistochemistry rat brains were extracted, washed with PBS and fixed in 4% paraformaldehyde (PFA) for 3 h. After fixation brains were embedded in FSC22 compound (Leica biosystems), frozen in liquid nitrogen and stored at − 70 °C. Brains were sectioned to 20 µm thick slices on a freezing microtome CM1850UV (Leica biosystems). For immunoblotting analysis brains after extraction were immediately frozen in liquid nitrogen and homogenized using a cryogenic laboratory mill Freezer/Mill 6870 (SPEX SamplePrep).

Biochemical analysis of MBP aggregation

Homogenized brain tissue samples weighing 0.1 g were resuspended in 500 µl of TBS buffer (50 mM Tris–HCl, pH 7.6, 150 mM NaCl) with the addition of a Complete Protease Inhibitor Cocktail (Roche). Then, SDS solution was added to the lysates to a final concentration of 1%. After incubation for 15 min at room temperature, the detergent-treated lysates were centrifuged for 2 h (260,000*g*, 18 °C) in an Optima MAX-XP ultracentrifuge (Beckman Coulter) in a TLA-100 rotor. The sediment fraction containing SDS-resistant aggregates was suspended in a volume equal to the volume of the supernatant. The supernatant fraction was then centrifuged in

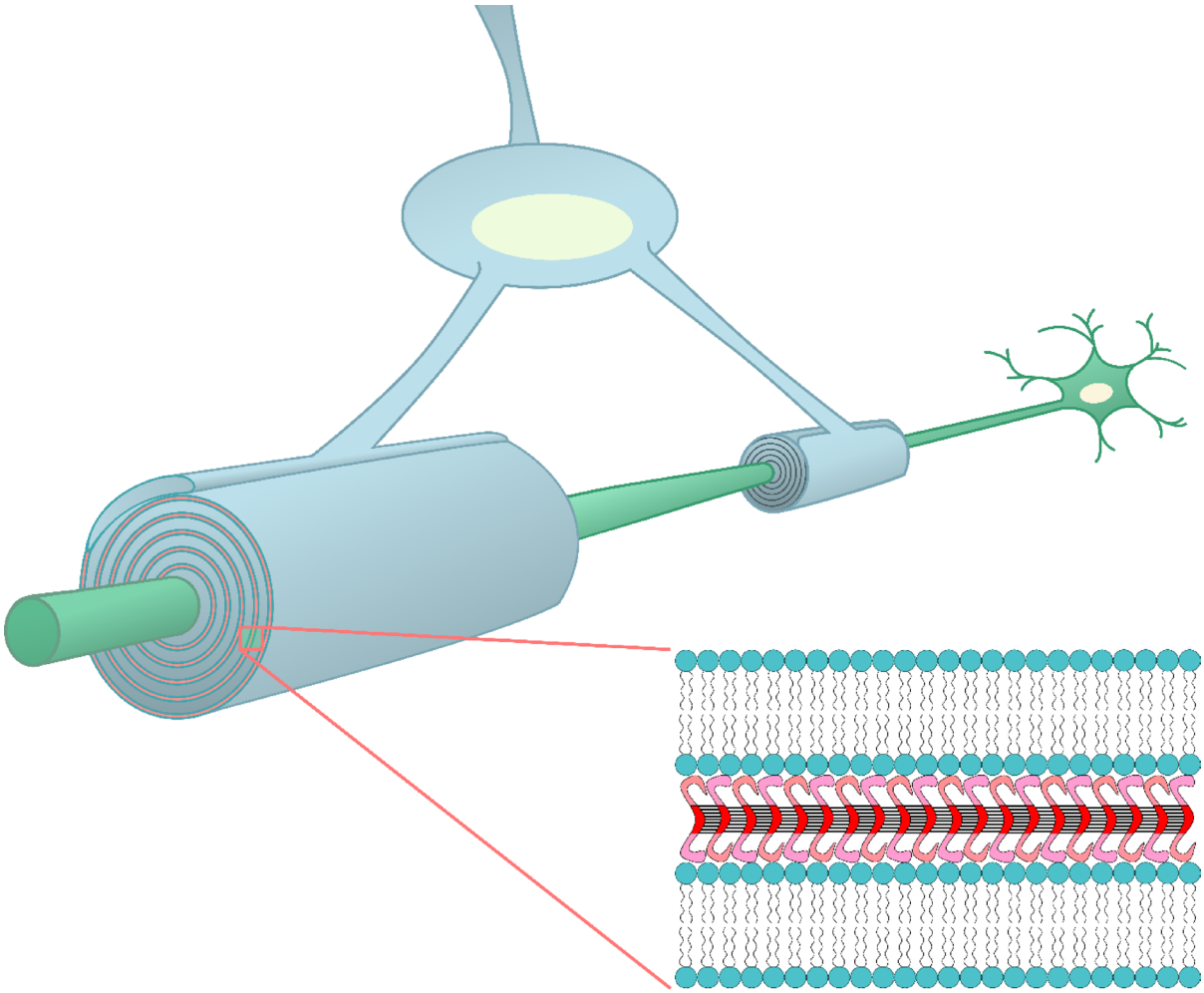

Fig. 6. Model of CNS myelin sheath structure. An oligodendrocyte forms flattened processes (blue) around the axons of neurons (green). The terminal parts of MBP (pink) bind to the lipids of the inner leaflets of the membranes, while its central region (red) is involved in the formation of cross-β-sheet. Black lines correspond to intermolecular hydrogen bonds.

an Eppendorf 5810 R centrifuge in an F-34–6-38 rotor for 20 min (4,000 g, 4 °C) through a concentrator filter with a pore diameter corresponding to a molecular weight of 30 kDa (Amicon Ultra-15). After centrifugation of each sample, the fraction of proteins with a molecular weight above 30 kDa remaining in the concentrator was also suspended in TBS in a volume equal to the volume of the monomer fraction solution (proteins with a molecular weight below 30 kDa). The resulting protein samples were then heated in SDS-PAGE loading buffer (4 × buffer: 100 mM Tris–HCl at pH 6.8, 20% 2-mercaptoethanol, 8% SDS, 0.2% bromophenol blue, 40% glycerol) for 15 min at 95 °C. Semi-denaturing detergent agarose gel electrophoresis (SDD-AGE)[18] was performed using 1% agarose gel. Before loading onto a gel, protein extracts were treated for 10 min with 1% SDS at room temperature. After SDS-PAGE and SDD-AGE the MBP protein was detected with monoclonal primary antibodies ab7349 (1:1500, Abcam, Cambridge, UK) and secondary Goat Anti-Rat IgG H&L (HRP) STAR72 (1:30,000, Bio-Rad, USA). Chemiluminescent detection was performed using the Amersham ECL Select Western Blotting Detection Reagent (GE Healthcare, USA).

Immunohistochemistry and immunoprecipitation

Immunohistochemistry and histological staining were performed on animals' brain cryosections. In preparation for the immunohistochemical study, 20 µm thick cryosections were incubated in 1% $NaBH_4$ for 10 min to reduce the level of background autofluorescence. Further, antigen retrieval was performed for cryosections of the brain of a grass frog, red-eared slider turtle, domestic chicken, and brown rat by incubation in 0.01 M citrate buffer with the addition of 0.05% Tween-20 for 10 min at 95 °C, followed by slow cooling to room temperature. All slides were then treated with 0.1% Triton X-100 in PBS for 20 min. At each stage the samples were washed three times with a PBS solution for 5 min. Further, to reduce nonspecific binding of antibodies, the preparations were incubated in 1% bovine serum albumin (BSA) in PBS buffer in the presence of 0.1% Tween-20 for 1 h at a temperature of 37 °C. The primary anti-MBP antibody ab7349 (1:100, Abcam, Cambridge, UK) and secondary antibody Goat anti-Rat IgG (H + L) conjugated with Alexa Fluor 647 or with Alexa Fluor 488 (ab150167 and

Primer name	Sequence
fMBP1HindIII	GATAAGCTTATGGCATCACGAAGAGAC
rMBP59BglII	TTAGATCTCTTGCCAGAGCCCCGCT
fMBP60HindIII	TATAAGCTTATGGTACCCTGGCTAAAGCAG
rMBP154BglII	TTAGATCTGCGTCTTGCCATGGGAGA
rMBP119BglII	TATAGATCTTGTCACAATGTTCTTGAATAA
fMBP86BglII	ATAAAGCTTATGGACTCACACACAAGAACTACC
rMBP60blunt	CTTGCCAGAGCCCCGCTTGG
fMBP105blunt	GATGAAAACCCAGTAGTAGTCCACTTCT

Table 1. Primers used in this work. The "f" and "r" symbols in the primers' names denote forward and reverse primers, correspondingly. The numbers in the primers' names are equal to numbers of first or last amino acid residues in corresponding MBP fragments.

ab150165, correspondingly, both 1:500, ThermoFisher Scientific, USA) were used. CR staining was done using 1% CR solution in 50% ethanol for 30 min. ThS staining was done using 1% ThS solution in 70% ethanol for 5 min.

For immunoprecipitation we used the method described previously[23] with modifications. Brain homogenate was incubated 20 min in lysis buffer (PBS, pH 7.4, 1 M NaCl) with the addition of a Complete Protease Inhibitor Cocktail (Roche). 1 M NaCl destroys protein complexes and removes proteins interacting with MBP fibrils. Then the lysate was diluted tenfold prior to immunoprecipitation. The anti-MBP antibodies ab7349 (1:25, Abcam, Cambridge, UK) were bound to 50 µl of protein G coated SileksMag-Protein G magnetic beads (Sileks, Moscow, Russia) according to manufacturer's protocol and incubated with animals' brain lysates for 2 h at room temperature. Protein samples were washed 12 times with PBS buffer containing 0.02% Tween. After incubation and washing, the protein sample was eluted with 200 µl of 0.1 M glycine buffer (pH 2.1) containing 1 M NaCl. The addition of sodium chloride prevents adhesion and non-specific interaction of proteins. The collected eluate was then neutralized by adding 40 µl 1.5 M Tris, pH 8.8. An aliquot of the eluate was boiled and analyzed by Coomassie gel staining and immunoblotting. MBP was detected with polyclonal primary antibodies PAA539Mi01 (1:3,000, Cloud-Clone, Wuhan, China) and secondary Goat Anti-Rabbit IgG H&L (HRP) ab205718 (1:20,000, Abcam, Cambridge, UK). Chemiluminescent detection was performed using the Amersham ECL Prime Western Blotting Detection Reagent (GE Healthcare, USA). The remaining portion of the protein sample was dialyzed (3.5 K MWCO Dialysis Tubing, Thermo Fisher Scientific) against PBS, then analyzed by immunolabeling followed by TEM or stained with CR.

Yeast and bacteria strains and growth conditions

The *E. coli* XL10-Gold strain (Tet^{r}Δ(*mcrA*)*183* Δ(*mcrCB-hsdSMR-mrr*)*173 endA1 supE44 thi-1 recA1 gyrA96 relA1 lac* Hte [F′ *proAB lacI^{q}ZΔM15* Tn*10* (Tet^r) Amy Cam^r]) (Stratagene) was cultivated at 37 °C on Luria–Bertani agar plates containing ampicillin for selection of transformants. The yeast *S. cerevisiae* strain GT409 (*MATa ade1–14$_{UGA}$ his3 leu2 lys2 trp1 ura3* [*psi$^-$*][*pin$^-$*])[33] was used for production of chimeric proteins containing MBP-YFP fusion. The rich organic medium (YEPD) and the selective yeast minimal synthetic medium (SD) with necessary supplements were used for culturing yeast cells. To study the aggregation of MBP fragments or its full-length isoforms fused with YFP, yeast transformants were grown on a selective medium lacking uracil with the addition of 100 µM $CuSO_4$ for 3 days. Before confocal microscopy yeast cells were precipitated from the culture medium by centrifugation at 3000*g* for 5 min, suspended in a drop of PBS and covered with a coverslip.

Plasmid construction

RNA from homogenized brain was isolated using TRIzol reagent (Thermo Fisher Scientific, USA) according to the manufacturer's protocol. cDNA synthesis using oligo(dT)$_{12–18}$ was performed with SuperScript III Reverse Transcriptase (Thermo Fisher Scientific, USA) according to the manufacturer's protocol. The obtained cDNA sequences encoding fragments of the MBP protein were amplified by PCR with according primers (Table 1). The sequence encoding MBP form with the 60-105 amino acid residues region deleted was obtained by direct ligation of the fragments encoding MBP(1–59) and MBP(106–154), followed by PCR amplification with primers fMBP1HindIII and rMBP154BglII (Table 1). The genes were then cloned into pJET 1.2 using a CloneJET PCR Cloning Kit (Thermo Fisher Scientific, USA) according to the manufacturer's protocol.

To analyze the aggregation of MBP fragments fused with the YFP in *S. cerevisiae* yeast cells, centromeric plasmids pU-CUP1-MBP(1–59)-YFP, pU-CUP1-MBP(60-154)-YFP, pU-CUP1-MBP(60-119)-YFP, pU-CUP1-MBP(86–119)-YFP, pU-CUP1-MBP(Δ60-105)-YFP, pU-CUP1-MBP(17.22 kDa)-YFP, and pU-CUP1-MBP(14 kDa)-YFP were constructed based on the pU-CUP1-YFP vector[34]. For this purpose, DNA fragments encoding fragments of the MBP protein and its two full-length isoforms were cloned into HindIII and BamHI sites of the pU-CUP1-YFP plasmid. Sanger sequencing was performed to validate the absence of significant mutations in any of the constructed plasmids. The pGPD-YFP(URA3) plasmid[35] which contains the *YFP* gene of *Aequorea victoria* was used as a control in yeast fluorescence experiments.

Preparation of yeast lysate and staining of MBP-YFP aggregates with Thioflavin S

Yeast transformants carrying plasmids pU-CUP1-MBP(60-119)-YFP and pU-CUP1-MBP(17.22 kDa)-YFP were grown on selective medium lacking uracil for 3 days. Yeast cells were harvested by centrifugation at 3,000 g for 5 min. Cells were resuspended on ice in 200 µL of cold lysis buffer (PBS supplemented with NaCl up to 1 M, 2 mM PMSF, and 4 mM DTT). An equal volume of glass beads (BioSpec Products, USA) was then added to the suspension, and the cells were disrupted using a FastPrep-24 benchtop homogenizer (MP Biomedicals) for 12 cycles. Each cycle was performed at 6.0 m/s for 20 s, with incubation on ice for at least 3 min between cycles. The crude lysate was transferred to a new tube and centrifuged at 4 °C, 805 g for 5 min using a Jouan CR3i centrifuge (Thermo Scientific, USA). The total protein lysate (supernatant) was transferred to a new tube. A 20 µL aliquot of the yeast cell lysate was placed on a Polysine microscope glass slide (ThermoFisher Scientific, USA), evenly spread across the surface, and dried at 37 °C. The dried lysates were stained with 50 µL of a 1% aqueous solution of ThS for 1 min at room temperature, washed three times with PBS supplemented with NaCl up to 1 M, and covered with a clean coverslip. The edges of the coverslip were sealed with nail polish. The slides were immediately analyzed using a TCS SP5 confocal laser-scanning microscope (Leica Microsystems, Germany) with "Leica Application Suite X 3.3.0.16799" software.

Fluorescence microscopy

The analysis of colocalization of the fluorescently labeled secondary antibodies bound to anti-MBP antibodies with the amyloid specific dyes on rat brain slices as well as examination of aggregation of MBP fragments and its full-length isoforms fused to the YFP in yeast cells was performed using a TCS SP5 confocal microscope (Leica Microsystems, Germany) and "Leica Application Suite X 3.3.0.16799" software. For excitation of fluorescent proteins, we used 514 nm argon laser for the YFP fusion proteins. The emission filters were 525–600 nm for the detection of YFP signal.

To analyze the amyloid properties of YFP-fused MBP(17.22 kDa) and MBP(60-119), yeast cell lysates expressing the respective constructs were prepared and stained with ThS as described above. To prevent overlap of YFP and ThS fluorescence signals, control lysates were used to optimize imaging conditions: non-transformed cells stained with ThS and transformed cells not stained with ThS. An argon laser with a wavelength of 514 nm and an intensity of 100% was used for YFP excitation, and 525–550 nm emission filters were used to detect the YFP signal. A laser with a wavelength of 405 nm and an intensity of 100% was used to excite ThS, and 420–480 nm emission filters were used to detect the ThS signal.

In vitro fibril formation and ThT assay

The MBP(60-119) peptide (Almabion, Voronezh, Russia) at a concentration of 50 µM was incubated in PBS (pH 7.4) containing 0.5 mM $MgCl_2$ for 5 days at 37 °C. Fibril formation was verified by TEM and CR staining. For ThT assay synthetic peptide MBP(60-119) at a concentration 0.7 µM was incubated with shaking for 2 days at 37 °C in PBS (pH 7.4) with 10 µM ThT. In the "seeding" experiments, preformed MBP(60-119) aggregates were added to the monomers in a ratio of 1/20. Signal detection was performed every 15 min at an excitation wavelength of 448 nm and an emission wavelength of 482 nm using CLARIOstar Plus (BMG LABTECH, Germany).

Congo red staining of fibrils

For polarization microscopy, the protein samples after immunoprecipitation or in vitro fibril formation assay were resuspended in 10 µl of water, spotted on a glass slide, and air-dried. Preparations were stained with 1% water solution of CR for 5 min at room temperature. The samples were washed with water and covered with a coverslip. Brightfield and polarization microscopy images were acquired using a polarizing microscope BIOLAR PI PZO equipped with a camera ToupCam UCMOS10000KPA and ToupView (×86) software.

Sample preparation for TEM and fibril immunolabeling

Negatively stained samples were prepared on copper grids coated with Formvar (TESKAN, Czech Republic). An aliquot of the in vitro-prepared fibril solution of the MBP peptide comprising amino acid residues 60 to 119, in a volume of 10 µl, was adsorbed onto the formvar-coated grid for 1 min, blotted, washed twice with 10 µl of water for 10 s each, and then stained with 10 µl of a 1% uranyl acetate solution (Electron Microscopy Sciences, USA) for 1 min. After removal of the uranyl acetate, the samples were air-dried.

To localize the antigen (MBP) in the fibril preparation obtained by immunoprecipitation from rat brain, the immunogold labeling method was used. An aliquot of the fibril solution in a volume of 10 µl was adsorbed onto the formvar-coated grid for 2 min and then washed with deionized water. Blocking was performed using a 1% solution of human serum albumin (HSA) in PBS for 15 min. The sample was then incubated with a solution of primary antibodies—Rabbit Anti-MBP PAA539Mi01 (1:300, Cloud-Clone, Wuhan, China)—in a 1% HSA solution for 1.5 h at room temperature. After three washes in PBS for 5 min each, the sample was treated with secondary gold-conjugated antibodies—Goat Anti-Rabbit IgG G7402 (1:10, Sigma-Aldrich, USA)—in a 1% HSA solution for 1.5 h at room temperature. This was followed by two washes with phosphate-buffered saline for 5 min each and four washes with deionized water for 3 min each. After thorough drying of the grid, it was stained with 10 µl of a 1% uranyl acetate solution (Electron Microscopy Sciences, USA) for 1 min.

Statistical analyses

The colocalization of MBP with CR and ThS was analyzed by Pearson correlation analysis using the Coloc 2 plugin of ImageJ v. 1.54f. software. The standard error of proportion (SEP) was used to analyze the aggregation frequencies of full-length MBP isoforms and its fragments. The curve for ThT assay data was modeled using the formula described previously[36]. The lag time (tlag) was determined as the time at which ThT fluorescence reaches 10% of the maximum amplitude, averaged over five measurements[37]. The statistical significance of

differences was determined using the Student's t-test. Model construction, comparisons and data visualization were performed using RStudio v. 2024.09.1 software.

Data availability

The nucleotide sequence generated during the current study has been deposited in the NCBI database under the accession number PV475463.1 and is available at https://www.ncbi.nlm.nih.gov/nuccore/PV475463.1/.

Received: 31 March 2025; Accepted: 24 July 2025
Published online: 08 August 2025

References

1. Geren, B. B. The formation from the schwann cell surface of myelin in the peripheral nerves of chick embryos. *Exp. Cell Res.* **7**, 558–562 (1954).
2. Zalc, B. The Acquisition of Myelin: A Success Story. in *Purinergic Signalling in Neuron-Glia Interactions* (eds. Chadwick, D. & Goode, J.) 15–21 (Novartis Foundation, London, 2008).
3. Bechler, M. E., Swire, M. & Ffrench-Constant, C. Intrinsic and adaptive myelination—A sequential mechanism for smart wiring in the brain. *Dev. Neurobiol.* **78**, 68–79 (2018).
4. Stadelmann, C., Timmler, S., Barrantes-Freer, A. & Simons, M. Myelin in the central nervous system: Structure, function, and pathology. *Physiol. Rev.* **99**, 1381–1431 (2019).
5. Knowles, J. K., Batra, A., Xu, H. & Monje, M. Adaptive and maladaptive myelination in health and disease. *Nat. Rev. Neurol.* **18**, 735–746 (2022).
6. Love, S. Demyelinating diseases. *J. Clin. Pathol.* **59**, 1151–1159 (2006).
7. Waxman, S. G. Axon-glia interactions: Building a smart nerve fiber. *Curr. Biol.* **7**, R406-410 (1997).
8. Hartline, D. K. & Colman, D. R. Rapid conduction and the evolution of giant axons and myelinated fibers. *Curr. Biol.* **17**, R29-35 (2007).
9. Boggs, J. M. Myelin basic protein: A multifunctional protein. *Cell. Mol. Life Sci.* **63**, 1945–1961 (2006).
10. Akiyama, K., Ichinose, S., Omori, A., Sakurai, Y. & Asou, H. Study of expression of myelin basic proteins (MBPs) in developing rat brain using a novel antibody reacting with four major isoforms of MBP. *J. Neurosci. Res.* **68**, 19–28 (2002).
11. Readhead, C. & Hood, L. The dysmyelinating mouse mutations shiverer (shi) and myelin deficient (shimld). *Behav. Genet.* **20**, 213–234 (1990).
12. Seiwa, C., Kojima-Aikawa, K., Matsumoto, I. & Asou, H. CNS myelinogenesis in vitro: Myelin basic protein deficient shiverer oligodendrocytes. *J. Neurosci. Res.* **69**, 305–317 (2002).
13. Bakhti, M., Aggarwal, S. & Simons, M. Myelin architecture: Zippering membranes tightly together. *Cell. Mol. Life Sci.* **71**, 1265–1277 (2014).
14. Raasakka, A. et al. Membrane association landscape of myelin basic protein portrays formation of the myelin major dense line. *Sci. Rep.* **7**, (2017).
15. Kattnig, D. R., Bund, T., Boggs, J. M., Harauz, G. & Hinderberger, D. Lateral self-assembly of 18.5-kDa myelin basic protein (MBP) charge component-C1 on membranes. *Biochim. Biophys. Acta Biomembr.* **1818**, 2636–2647 (2012).
16. Aggarwal, S. et al. Myelin membrane assembly is driven by a phase transition of myelin basic proteins into a cohesive protein meshwork. *PLoS Biol.* **11**, (2013).
17. Sopova, J. V. et al. RNA-binding protein FXR1 is presented in rat brain in amyloid form. *Sci. Rep.* **9**, (2019).
18. Bagriantsev, S. N., Kushnirov, V. V. & Liebman, S. W. Analysis of amyloid aggregates using agarose gel electrophoresis. *Methods Enzymol.* **412**, 33–48 (2006).
19. Siniukova, V., Galkina, S. & Galkin, A. Thioflavin S binds non-amyloid protein structures in lampbrush chromosomes of Gallus gallus domesticus. *Biol. Commun.* **67**, 57–62 (2022).
20. Buxbaum, J. N. et al. Amyloid nomenclature 2024: Update, novel proteins, and recommendations by the International Society of Amyloidosis (ISA) Nomenclature Committee. *Amyloid* **31**, 249–256 (2024).
21. Jahn, O., Tenzer, S. & Werner, H. B. Myelin proteomics: Molecular anatomy of an insulating sheath. *Mol. Neurobiol.* **40**, 55–72 (2009).
22. Matiiv, A. B. et al. Structure and polymorphism of amyloid and amyloid-like aggregates. *Biochem.* **87**, 450–463 (2022).
23. Belashova, T. A. et al. Search and identification of amyloid proteins. *Methods Protoc.* **6**, (2023).
24. Tsolis, A. C., Papandreou, N. C., Iconomidou, V. A. & Hamodrakas, S. J. A Consensus method for the prediction of 'Aggregation-Prone' peptides in globular proteins. *PLoS One* **8**, (2013).
25. Ahmed, A. B. & Kajava, A. V. Breaking the amyloidogenicity code: Methods to predict amyloids from amino acid sequence. *FEBS Lett.* **587**, 1089–1095 (2013).
26. Fitzner, D. et al. Myelin basic protein-dependent plasma membrane reorganization in the formation of myelin. *EMBO J.* **25**, 5037–5048 (2006).
27. Bezsonov, E. E. et al. Amyloidogenic peptides of yeast cell wall glucantransferase Bgl2p as a model for the investigation of its pH-dependent fibril formation. *Prion* **7**, 175–184 (2013).
28. Ryzhova, T. A. et al. Screening for amyloid proteins in the yeast proteome. *Curr Genet.* **64**, 469–478 (2018).
29. Sergeeva, A. V. et al. Amyloid properties of the yeast cell wall protein Toh1 and its interaction with prion proteins Rnq1 and Sup35. *Prion* **13**, 21–32 (2019).
30. Kollmer, M. et al. Cryo-EM structure and polymorphism of Aβ amyloid fibrils purified from Alzheimer's brain tissue. *Nat. Commun.* **10**, (2019).
31. Guerrero-Ferreira, R. et al. Cryo-EM structure of alpha-synuclein fibrils. *Elife* **7**, (2018).
32. Maji, S. K., Wang, L., Greenwald, J. & Riek, R. Structure-activity relationship of amyloid fibrils. *FEBS Lett.* **583**, 2610–2617 (2009).
33. Allen, K. D. et al. Hsp70 chaperones as modulators of prion life cycle. Novel effects of Ssa and Ssb on the Saccharomyces cerevisiae Prion [PSI+]. *Genetics* **169**, 1227–1242 (2005).
34. Antonets, K. S., Sargsyan, H. M. & Nizhnikov, A. A. A glutamine/asparagine-rich fragment of Gln3, but not the full-length protein, aggregates in *Saccharomyces cerevisiae*. *Biochem.* **81**, 407–413 (2016).
35. Rubel, A. A. et al. Identification of PrP sequences essential for the interaction between the PrP polymers and Aβ peptide in a yeast-based assay. *Prion* **7**, 469–476 (2013).
36. Spiess, A. N., Feig, C. & Ritz, C. Highly accurate sigmoidal fitting of real-time PCR data by introducing a parameter for asymmetry. *BMC Bioinform.* **9**, (2008).
37. Arosio, P., Knowles, T. P. J. & Linse, S. On the lag phase in amyloid fibril formation. *Phys. Chem. Chem. Phys.* **17**, 7606–7618 (2015).

Acknowledgements

The authors acknowledge A.V. Radaev, M.G. Vorobiev, E.J. Gorodilova, A.A. Zelinsky, S.A. Galkina, and A.

Guseva for technical assistance. Special thanks to Alexey Zhigulin (Sileks, Russia) for advice on immunoprecipitation technique. The authors acknowledge St. Petersburg State University for the opportunity to use the facilities of the Resource Centers for Molecular and Cell Technologies and Chromas Core Facility. We are also grateful to N.R. Skrynnikov (SPbSU, Russia) for providing the mill Freezer/Mill 6870 (SPEX SamplePrep), G.A. Zhuravleva and S.A. Bondarev for providing the multi-mode plate reader CLARIOstar Plus.

Author contributions

E.I.S. conducted the experiments, wrote the manuscript, and prepared all figures. A.A.S., T.A. B., and S.P.Z. conducted the experiments. A.A.V. conducted the experiments, wrote the manuscript, and prepared a figure. A.P.G. conceptualized the study and wrote the manuscript. All authors reviewed the manuscript.

Funding

This work was supported by a grant from the Russian Science Foundation # 24-14-00233 to A.P.G.

Declarations

Competing interests

The authors declare no competing interests.

Additional information

Supplementary Information The online version contains supplementary material available at https://doi.org/10.1038/s41598-025-13524-z.

Correspondence and requests for materials should be addressed to A.P.G.

Reprints and permissions information is available at www.nature.com/reprints.

Publisher's note Springer Nature remains neutral with regard to jurisdictional claims in published maps and institutional affiliations.